Published in final edited form as:

Dev Neurosci. 2022 ; 44(6): 671–677. doi:10.1159/000525039.

Perineuronal Nets Degradation and Parvalbumin Interneuron loss in a Mouse Model of DEPDC5-related Epilepsy

Tao Yang[1], **Shuntong Hu**[1], **Wei-Chih Chang**[1], **Hsin-Yi Kao**[1], **Yu Wang**[1]

[1]Department of Neurology, University of Michigan, Ann Arbor, MI, U.S.A

Abstract

DEPDC5, the key gene within the mechanistic target of rapamycin (mTOR) pathway, is one of the most common causative genes in patients with epilepsy and malformation of cortical development (MCD). Although somatic mutations in the dorsal cortical progenitors generate the malformed cortex, its pathogenesis of hyperexcitability is complex and remains unclear. We specifically deleted *Depdc5* in the mouse forebrain dorsal progenitors to model DEPDC5-related epilepsy, and investigated whether and how parvalbumin interneurons were non-cell autonomously affected in the malformed cortex. We showed that long before seizures, coincident with microglia inflammation, proteolytic enzymes degraded perineuronal nets (PNN) in the malformed cortex, resulting in parvalbumin (PV+) interneuron loss and presynaptic inhibition impairment. Our studies therefore uncovered the hitherto unknown role of PNN in mTOR-related MCD, providing a new framework for mechanistic-based therapeutic development.

Keywords

malformation of cortical development; perineuronal nets; epilepsy

Introduction

As the key gene in the mTOR signaling pathway, *DEPDC5* mutations have been frequently discovered in epilepsy patients with MCD, including focal cortical dysplasia type II (FCDII), hemi-megalencephaly (HMEG), and megalencephaly (MEG) [1]. The conceptual paradigm in MCD is somatic mutations in dorsal cortical progenitors disrupt the normal neurodevelopment, yielding a focal malformation as the pathological substrate for seizures [2]. However, the pathogenic and epileptogenic mechanisms could be more complex. For example, mutant excitatory neurons generated by dorsal progenitors are cytomegalic,

CORRESPONDING AUTHOR: Yu Wang, MD, PhD, Assistant Professor, Department of Neurology, University of Michigan, Address: 5025 BSRB, 109 Zina Pitcher Place, Ann Arbor, MI, USA, 48109-2200, Tel: 860-942-3293, eegwang@med.umich.edu.

AUTHOUR CONTRIBUTION

Tao Yang and Yu Wang designed the study. Tao Yang, Shuntong Hu, Hsin-Yi Kao, and Wei-Chih Chang performed the experiments. Tao Yang, Shuntong Hu, Hsin-Yi Kao, Wei-Chih Chang, and Yu Wang analyzed the data. Tao Yang, Shuntong Hu, and Yu Wang interpreted the data, wrote and edited the manuscript.

STATEMENT OF ETHICS

The study was approved by the University of Michigan Institutional Animal Care and Use Committee (IACUC), approval number PRO00010265.

CONFLICT OF INTEREST

The authors have declared that no conflict of interest exists.

and whether these mutant cells are hyperexcitable remains unclear and controversial[3], suggesting that they alone cannot cause a hyperexcitable network. Interestingly, the reduction of the interneuron number and the impairment of presynaptic inhibitory transmission were also observed[4], explaining the excitation-inhibition imbalance. However, because interneurons are generated in ventral ganglionic eminences that are anatomically and developmentally distant from dorsal progenitors, they are not affected by somatic mutation events in dorsal progenitors that give rise to MCD.

It is then intriguing whether and how these wild-type interneurons are impaired. To answer these questions, we first generated a mouse model of DEPDC5-related epilepsy by deleting *Depdc5* specifically in the forebrain dorsal progenitors. These mice were megalencephalic and developed severe seizures, recapitulating the clinical features of mTOR-related MCD. We then identified that long before seizures, coincident with Iba1+ microglial activation, excessive release of matrix metalloproteinases (MMP) degraded protective PNN, resulting in PV+ interneuron loss and impaired presynaptic inhibition. Therapeutically, mTOR inhibition prevented PNN degradation, PV+ cell loss, and seizures. Our studies, therefore, provided a new framework to investigate the pathogenesis of Depdc5-related epilepsy at molecular, cellular, and circuitry levels. The disruption of PNNs may account for hyperexcitability in mTOR-related epilepsies, and PNN protection may provide therapeutic benefits.

Materials and Methods

Animals

Mouse experiments were performed in a mixed-strain background using both male and female mice. All mice were housed in a 12-hr light-dark cycle, climate-controlled room, with access to food and water ad-lib. Dr. Jun Hee Lee at the University of Michigan provided *Dedpc5*$^{F/F}$ mice that were originated from the HEPD0734_3_G10 embryonic stem cell clone and obtained from the European Mouse Mutant Archive[5]. This transgenic line contained a floxed-stop allele of exon 5 (*Depdc5*$^{tm1c(EUCOMM)Hmgu}$) and was also characterized previously by other groups[6, 7]. Emx1-Cre mice (Jackson Laboratories, stock #005628) and were used to delete *Depdc5* specifically in the forebrain dorsal progenitors. To mitigate the risk of germline transmission, male homozygous *Depdc5* conditional mice (*Depdc5*$^{F/F}$) were bred with female heterozygous for *Depdc5* (*Depdc5*$^{F/w}$) and Emx1-Cre to generate litters of homozygous CKO *Depdc5*$^{F/F}$; Emx1-Cre(referred to herein as CKO), heterozygous *Depdc5*$^{F/W}$; Emx1-Cre (referred to herein as *Depdc5*^{Emx1} het), *Depdc5*$^{F/F}$and *Depdc5*$^{F/W}$ mice (referred to herein as wildtype, WT). Pvalb-tdTomato mice (Jackson Laboratories #028594) were used to label parvalbumin-positive interneurons. All animal procedures were approved by the IACUC of University of Michigan.

Genotyping, immunohistochemistry, western blot

Please see the full description in Supplementary Material 1 file.

EEG implantation and analysis

P16~18 mice with three epidural screw electrodes were monitored for 8 hours per day and then returned to the mother. Procedures for affixing electrodes in young rodents were

performed as we previously described[8]. To detect the earliest seizures, a subset of <P14 mice were monitored for 3 hours, two times every day, and then returned to the mother.

Acute slice electrophysiology, in situ Zymography, and Everolimus treatment

Please see the full description in the supplementary file.

Quantification and statistical analysis

Images were acquired by Nikon A1 inverted confocal microscope. Quantification was performed on images obtained from somatosensory cortex. PV+, WFA+, and Iba1+ cells were counted throughout all six layers of the somatosensory cortex with a width of 635 μm. The soma size of NeuN labeled pyramidal neurons was measured in ImageJ software. The arbitrary unit (AU) of WFA immunoreactivity surrounding interneurons and in the background was directly measured by ImageJ. The relative signal strength was calculated as: (the interneuron WFA AU - the background AU)/the background AU. The relative signal strength of *in situ* Zymography assays was calculated similarly.

All data measurements were kept in Excel (Microsoft, Redmond, WA). All data were analyzed in GraphPad Prism v8.2. We ensured data were normally distributed in statistical tests, such as Kolmogorov–Smirnov normality tests. p values were determined by the student t-test. Analysis of variance was conducted with Bonferroni post hoc correction for multiple comparisons. All data were shown as mean ± s.e.m. A p-value less than 0.05 was considered to be statistically significant. In figure panels throughout the manuscript, the following labeling conventions for statistical testing are used: NS, $p>0.05$; *, $p<0.05$; **, $p<0.01$; ***, $p<0.001$; ****, $p<0.0001$.

Results

Depdc5 deletion in the forebrain dorsal progenitors generates megalencephaly and severe epilepsy

We deleted *Depdc5* gene in the developing forebrain by crossing *Depdc5* floxed mice to *Emx1*-Cre mice that specifically express Cre recombinase in dorsal progenitors at embryonic day (E) 10.5 [9] (Suppl. Fig.1A). The dissected cortex from *Depdc5*$^{F/F}$; *Emx1*-Cre$^{+/-}$ mice (hereafter CKO) brain showed almost a complete loss of Depdc5 protein on Western blot at postnatal day (P) 1 (Suppl. Fig. 1B)., Phosphorylated S6 (pS6) (s240/244), the hallmark of mTOR hyperactivation, was significantly increased (Suppl. Fig. 1B–D). CKO were megalencephalic and showed increased cortical thickness (Suppl. Fig. 1C–E). Cortical excitatory neurons in CKO were cytomegalic and showed increased surface area (Suppl. Fig. 1F). EEG implantation on P16~18 mice was performed for seizure characterization (Suppl. Fig. 1G, H, K–M). A subset of animals (P<14) underwent serial video EEG monitoring to determine the seizures onset (Suppl. Fig.1J). Because of technical difficulties of EEG recoring on young immature animals (<P14), particularly on these fragile *Depdc5* CKO mice, the number of animals that successfully completed serial EEG monitoring was limited (n=3). No seizures were detected prior to P15. Interestingly, CKO had normal early postnatal development but began to die after P15 (Suppl. Fig. 1I),

suggesting sudden unexpected death in epilepsy (SUDEP)-like events. As shown previously, *Depdc5* heterozygous CKO had normal development and showed no phenotypes[6, 10].

PNN degradation and PV+ interneurons loss in the malformed cortex

Because somatic inhibition on excitatory neurons is primarily mediated by PV+ interneurons, the most abundant neocortical interneurons, we used wisteria floribunda agglutinin (WFA) and parvalbumin (PV) antibody staining to examine if they are affected. WFA stains perineuronal nets (PNN) surrounding ~80% of PV+ interneurons [11]. Unexpectedly, both the intensity and density of WFA immunostaining were significantly decreased (Fig. 1A, C) in CKO. Serial WFA staining showed that PNN started degradation at P8, long before P15 when animals started developing seizures (Fig. 1E). Concurrently, the number and density of PV+ cells decreased by ~35.8% and 44%, respectively (Fig. 1B, D). Brain slice recording on P15 animals showed CKOs had fewer miniature inhibitory postsynaptic currents (mIPSC) with longer inter-event intervals on pyramidal neurons (Fig. 1F–G).

In situ zymography gelatinase assay showed the enzymatic activity of MMP-2 and MMP-9 (DQG/gelatinase), two major MMP capable of degrading aggrecan-enriched PNN, was significantly increased on CKO brain slices (Fig. 1H, I). Because pathologically activated microglia are known contributors to MMP secretion[12], we analyzed the expression of Iba1+ microglia in the malformed cortex. The density of microglia was not different between WT and CKO (data not shown) at P8 and P16. Interestingly, most Iba1+ microglia in CKO were in the activated state with an amoeboid or bushy morphology (Fig. 1J–L), while most Iba1+ cells in WT were in the resting state. These data suggested that the microenvironment in the malformed cortex entailed a marked shift toward microglia activation.

Early treatment with Everolimus rescues PNN degradation, PV+ interneuron loss, and seizures

We next administered Everolimus, a potent mTOR inhibitor, to CKO from P8 when PNN started degradation but before animals developed seizures. This early treatment prevented PNN degradation, PV+ cell loss (Fig. 2A–C, F, G) as well as mTOR hyperactivation, megalencephaly, cytomegaly (Fig. 2D, E), and microglial activation (Fig. 2H–K). EEG studies showed the near absence of interictal discharges, and only one treated CKO mice had rare seizures.

Clinically, patients with mTOR-related MCD, for example, tuberous sclerosis complex (TSC), receive mTOR inhibitor treatment after years of seizures and rarely achieve seizure-free. Therefore, we performed a late treatment experiment during which Everolimus was started at P16~P18 after animals had already developed seizures. Surprisingly, the late treatment still rescued premature death, and all animals survived well into at least P30. Although seizures were still present, there was a significant reduction (0.176±0.02 sz/hr in vehicle treatment group, n=6, vs. 0.0532±0.058 sz/hr in Everolimus group, n=5. p=0.0010, student *t*-test). Although interneuron loss could not be completely rescued, the severity was less severe as compared to non-treated animals (Fig. 2O). Interestingly, the signal strength of

PNN staining in late-treatment CKO was similar to that in WT animals (Fig. 2N). These data suggested that late treatment could not rescue PNN degradation/PV+ cell loss that already existed before the treatment but could prevent ongoing deterioration and disease progression.

Discussion

When *Depdc5* was deleted in post-mitotic excitatory and interneurons at the entire nervous system level, mice only had rare seizures during adulthood [6]. In contrast, our dorsal progenitor-specific deletion resulted in an early-onset (~P15) severe epileptic phenotype. The much milder epileptic phenotype raised an interesting question of whether interneuron or other neuronal subtypes with mTOR hyperactivation could be protective. Interestingly, several large cohort studies did not identify somatic mutations in interneurons in mTOR-related MCD[13]. Experimentally, expression of *PIK3CA* p.H1047R, a mutation associated with both FCD and HME, in ventral progenitors that give rise to interneurons did not generate megalencephaly and seizures[13].

PNN degradation in the malformed cortex occurred long before animals developed their seizures, suggesting they were not caused by secondary injury from frequent seizures. PNN not only supports the fast-spiking physiology of PV+ interneurons but protects them from oxidative stress and excitotoxicity. Pathological PNN degradation causes PV+ cell loss in several neurological disorders[14]. For example, PNN degradation was associated with PV+ cell loss and compromised the GABAergic inhibition in the peritumoral region, contributing to epileptiform activities in tumor-associated epilepsy[11]. Consistent with PNN degradation, Gelatinase assays demonstrated that the malformed cortex had significantly increased enzymatic activity of MMP[11], particularly MMP9 and 2, that cleaves aggrecan-enriched PNN [12]. An alternative hypothesis for PV+ cell loss is that mutated excitatory neurons, via activity-dependent survival mechanisms, could affect the ultimate number of inhibitory cells [15]. However, an increased interneuron number would be expected in the hyperexcitable cortex, and early-life seizures significantly increase PNN expression during brain development[16].

Our study also showed that pathologically activated microglia, the primary source of MMP[17] and the facilitator of PNN degradation[18], were also markedly increased long before seizures. As the primary innate immune cells in the brain, microglia continuously survey their surrounding micro-environmental milieu and are being activated in response to diseased states[19]. In the malformed cortex, mutant excitatory neurons are cytomegalic and have severely disrupted cellular homeostasis, such as autophagy blockage (data now shown). Therefore, these mutant cells could activate surrounding microglial cells and elicit an inflammatory response. In addition, mTOR inhibitor rescued microglial activation, PNN degradation, and PV+ cell loss and prevented seizures, suggesting that these pathological findings highly correlate with, and/or at least in part contribute to the hyperexcitability in the malformed cortex.

The efficacy of Everolimus is more pronounced in younger children than in the older subgroup[20], consistent with the difference between our early and late Everolimus treatment. In the late treatment group, PV+ cell loss was not completely rescued but

the severity was significantly improved. Along with the normal WFA staining, these data suggested late treatment could not rescue the PV+ cell loss that had already existed but could prevent ongoing PNN degradation. Early intervention with Everolimus is therefore important for the treatment of mTOR-related epilepsy. Therapeutic development to enhance interneuron-mediated inhibition or to protect PNN should also be investigated in the future.

Supplementary Material

Refer to Web version on PubMed Central for supplementary material.

ACKNOWLEDGEMENT

We thank Dr. Jun Hee Lee for donating the *Depdc5*$^{Flox/Flox}$ transgenic mice.

FUNDING SOURCES

Yu Wang received support from NIH (R01NS113824 and U54NS117170)

DATA AVAILABILITY STATEMENT

All data generated or analysed during this study are included in this article. Further enquiries can be directed to the corresponding author.

REFERENCES

1. Baldassari S, Picard F, Verbeek NE, van Kempen M, Brilstra EH, Lesca G, et al. The landscape of epilepsy-related GATOR1 variants. Genet Med. 2019 Feb;21(2):398–408. [PubMed: 30093711]
2. Poduri A, Evrony GD, Cai X, Walsh CA. Somatic mutation, genomic variation, and neurological disease. Science. 2013 Jul 5;341(6141):1237758. [PubMed: 23828942]
3. Koh HY, Jang J, Ju SH, Kim R, Cho GB, Kim DS, et al. Non-Cell Autonomous Epileptogenesis in Focal Cortical Dysplasia. Ann Neurol. 2021 Aug;90(2):285–99. [PubMed: 34180075]
4. Calcagnotto ME, Paredes MF, Tihan T, Barbaro NM, Baraban SC. Dysfunction of synaptic inhibition in epilepsy associated with focal cortical dysplasia. J Neurosci. 2005 Oct 19;25(42):9649–57. [PubMed: 16237169]
5. Cho CS, Kowalsky AH, Namkoong S, Park SR, Wu S, Kim B, et al. Concurrent activation of growth factor and nutrient arms of mTORC1 induces oxidative liver injury. Cell Discov. 2019;5:60. [PubMed: 31754457]
6. Yuskaitis CJ, Jones BM, Wolfson RL, Super CE, Dhamne SC, Rotenberg A, et al. A mouse model of DEPDC5-related epilepsy: Neuronal loss of Depdc5 causes dysplastic and ectopic neurons, increased mTOR signaling, and seizure susceptibility. Neurobiol Dis. 2018 Mar;111:91–101. [PubMed: 29274432]
7. Klofas LK, Short BP, Snow JP, Sinnaeve J, Rushing GV, Westlake G, et al. DEPDC5 haploinsufficiency drives increased mTORC1 signaling and abnormal morphology in human iPSC-derived cortical neurons. Neurobiol Dis. 2020 Sep;143:104975. [PubMed: 32574724]
8. Kao HY, Hu S, Mihaylova T, Ziobro J, Ahn E, Fine C, et al. Defining the latent period of epileptogenesis and epileptogenic zone in a focal cortical dysplasia type II (FCDII) rat model. Epilepsia. 2021 May;62(5):1268–79. [PubMed: 33735460]
9. Gorski JA, Talley T, Qiu M, Puelles L, Rubenstein JL, Jones KR. Cortical excitatory neurons and glia, but not GABAergic neurons, are produced in the Emx1-expressing lineage. J Neurosci. 2002 Aug 1;22(15):6309–14. [PubMed: 12151506]
10. Klofas LK, Short BP, Zhou C, Carson RP. Prevention of premature death and seizures in a Depdc5 mouse epilepsy model through inhibition of mTORC1. Hum Mol Genet. 2020 May 28;29(8):1365–77. [PubMed: 32280987]

11. Tewari BP, Chaunsali L, Campbell SL, Patel DC, Goode AE, Sontheimer H. Perineuronal nets decrease membrane capacitance of peritumoral fast spiking interneurons in a model of epilepsy. Nat Commun. 2018 Nov 9;9(1):4724. [PubMed: 30413686]
12. Crapser JD, Ochaba J, Soni N, Reidling JC, Thompson LM, Green KN. Microglial depletion prevents extracellular matrix changes and striatal volume reduction in a model of Huntington's disease. Brain. 2020 Jan 1;143(1):266–88. [PubMed: 31848580]
13. D'Gama AM, Woodworth MB, Hossain AA, Bizzotto S, Hatem NE, LaCoursiere CM, et al. Somatic Mutations Activating the mTOR Pathway in Dorsal Telencephalic Progenitors Cause a Continuum of Cortical Dysplasias. Cell Rep. 2017 Dec 26;21(13):3754–66. [PubMed: 29281825]
14. Wen TH, Binder DK, Ethell IM, Razak KA. The Perineuronal 'Safety' Net? Perineuronal Net Abnormalities in Neurological Disorders. Front Mol Neurosci. 2018;11:270. [PubMed: 30123106]
15. Wong FK, Bercsenyi K, Sreenivasan V, Portales A, Fernandez-Otero M, Marin O. Pyramidal cell regulation of interneuron survival sculpts cortical networks. Nature. 2018 May;557(7707):668–73. [PubMed: 29849154]
16. McRae PA, Baranov E, Sarode S, Brooks-Kayal AR, Porter BE. Aggrecan expression, a component of the inhibitory interneuron perineuronal net, is altered following an early-life seizure. Neurobiol Dis. 2010 Sep;39(3):439–48. [PubMed: 20493259]
17. Konnecke H, Bechmann I. The role of microglia and matrix metalloproteinases involvement in neuroinflammation and gliomas. Clin Dev Immunol. 2013;2013:914104. [PubMed: 24023566]
18. Crapser JD, Spangenberg EE, Barahona RA, Arreola MA, Hohsfield LA, Green KN. Microglia facilitate loss of perineuronal nets in the Alzheimer's disease brain. EBioMedicine. 2020 Aug;58:102919. [PubMed: 32745992]
19. Nimmerjahn A, Kirchhoff F, Helmchen F. Resting microglial cells are highly dynamic surveillants of brain parenchyma in vivo. Science. 2005 May 27;308(5726):1314–8. [PubMed: 15831717]
20. Curatolo P, Franz DN, Lawson JA, Yapici Z, Ikeda H, Polster T, et al. Adjunctive everolimus for children and adolescents with treatment-refractory seizures associated with tuberous sclerosis complex: post-hoc analysis of the phase 3 EXIST-3 trial. Lancet Child Adolesc Health. 2018 Jul;2(7):495–504. [PubMed: 30169322]
21. Nayak D, Roth TL, McGavern DB. Microglia development and function. Annu Rev Immunol. 2014;32:367–402. [PubMed: 24471431]

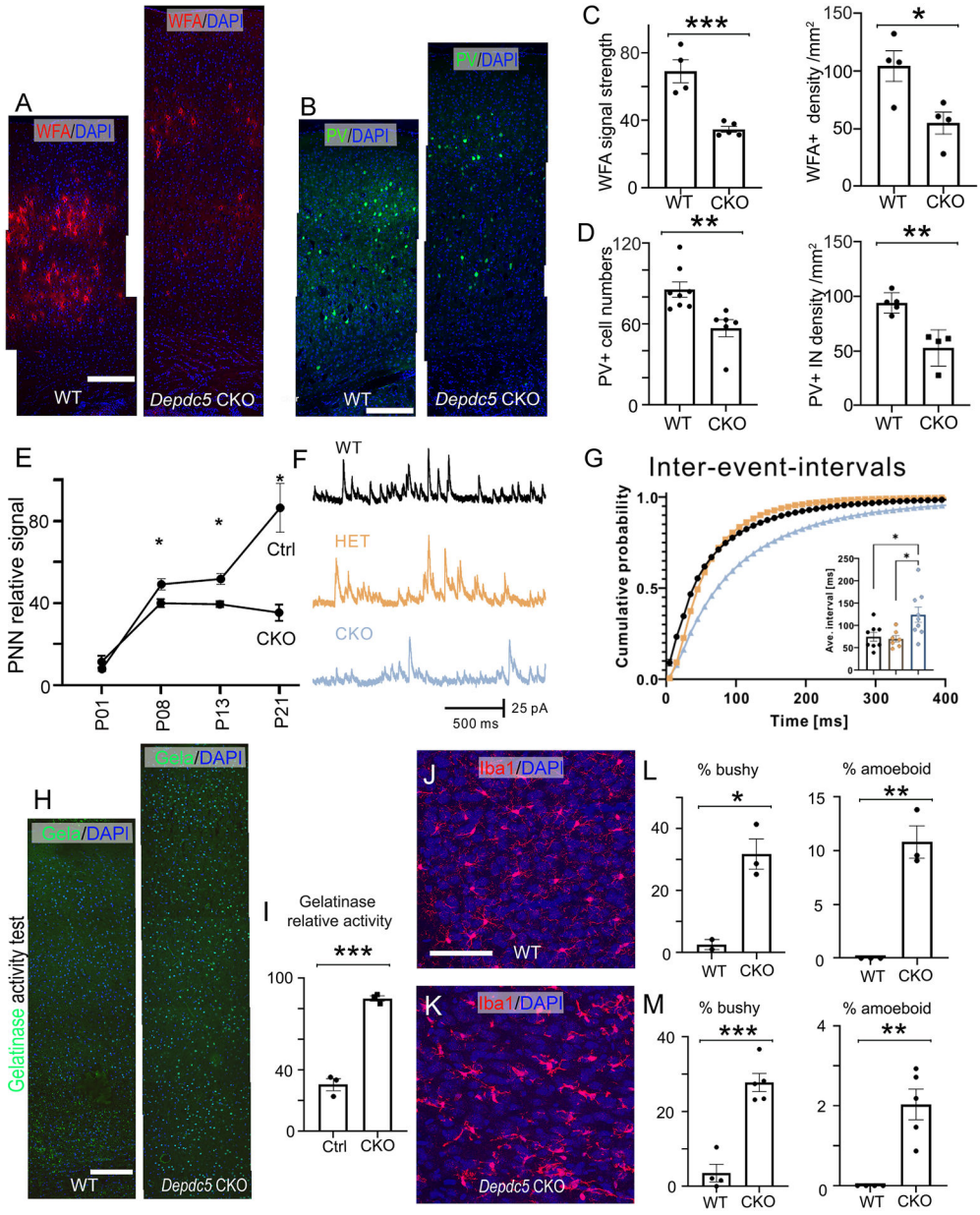

Figure 1. PNN degradation and PV+ cell loss in the malformed cortex.

A, B) Shown are representative images of WFA A) and PV antibody staining B) in WT and CKO mice. C) Quantification of WFA+ relative immunofluorescent intensity (WT vs. CKO: 69.1±6.82 vs. 34.5±3.9; n≥14 WFA cells per animal from 5 CKO and 4 WT) and density. D) Quantification of the total number of PV+ cells (WT vs. CKO: 88.5±7.0 vs. 56.8±6.4 PV+ cells in the somatosensory cortex with 635 μm width; 6 CKO and 8 WT) and PV+ cell density (WT vs. CKO: 94.1±4.1 vs. 52.7±8.4 PV+ cells /mm^2; 4 CKO and 6 WT) are decreased in CKO. E) Relative WFA signal strength starts decreasing at P8 (WT vs. CKO: P1: 8.0±2.41 vs.11.5±5.9, n=4 from each group, p=0.31; P8: 49.3±5.3 vs. 40.1±3.4, n=3 in CKO and 4 in WT; P13: 51.9±5.3 vs. 39.6±2.4, n=3 in each group; P21: 86.1±20.4 vs. 35.4±6.6, n=3 in each group). F) Shown are representative images of miniature IPSCs

(mIPSCs) recorded from the pyramidal neurons of WT (black trace), Het (orange trace), and CKO (the blue trace) mice. G) The cumulative probabilities of the inter-event-intervals and the inset shows the average inter-event-intervals (8 WT cells, 7 Het cells, and 9 CKO cells from at least three animals in each group. WT 74.58±9.91 ms vs. HET, 69.69±7.09 ms vs. CKO, 123.8±16.87ms). H) Representative images show gelatinase activity (DQG-green) in the cortex of WT and CKO animals. I) Mean relative gelatinase activity in WT: 30.6±6.8 vs. CKO: 86.9±3.1. Ctrl n = 3, CKO n=3. J, K) Representative images of Iba1 staining in the cortex of WT J) and CKO K). Resting microglia are characterized by a small cell body and elaborated thin processes with multiple branches extending in all directions. In contrast, activated microglia have a larger cell body with shorter and thick processes or a rod-shaped amoeboid-like morphology[21]. L) Quantification of activated microglia cells at J) P8 prior to the development seizures (31.9±6.4% bushy and 10.8±1.5% amoeboid-like microglia in CKO vs. 2.7±1.8% bushy and a near absence of amoeboid-like microglia in WT. N=3 in WT and CKO=3), and at M) P16 (27.7±5.5% bushy and 2.0±1.0% amoeboid-like microglia in CKO vs. 3.5±1.0% bushy and no amoeboid-like microglia in WT. 4 WT and 5 CKO). Scale bar in A and H: 200 μm, in B: 100 μm.

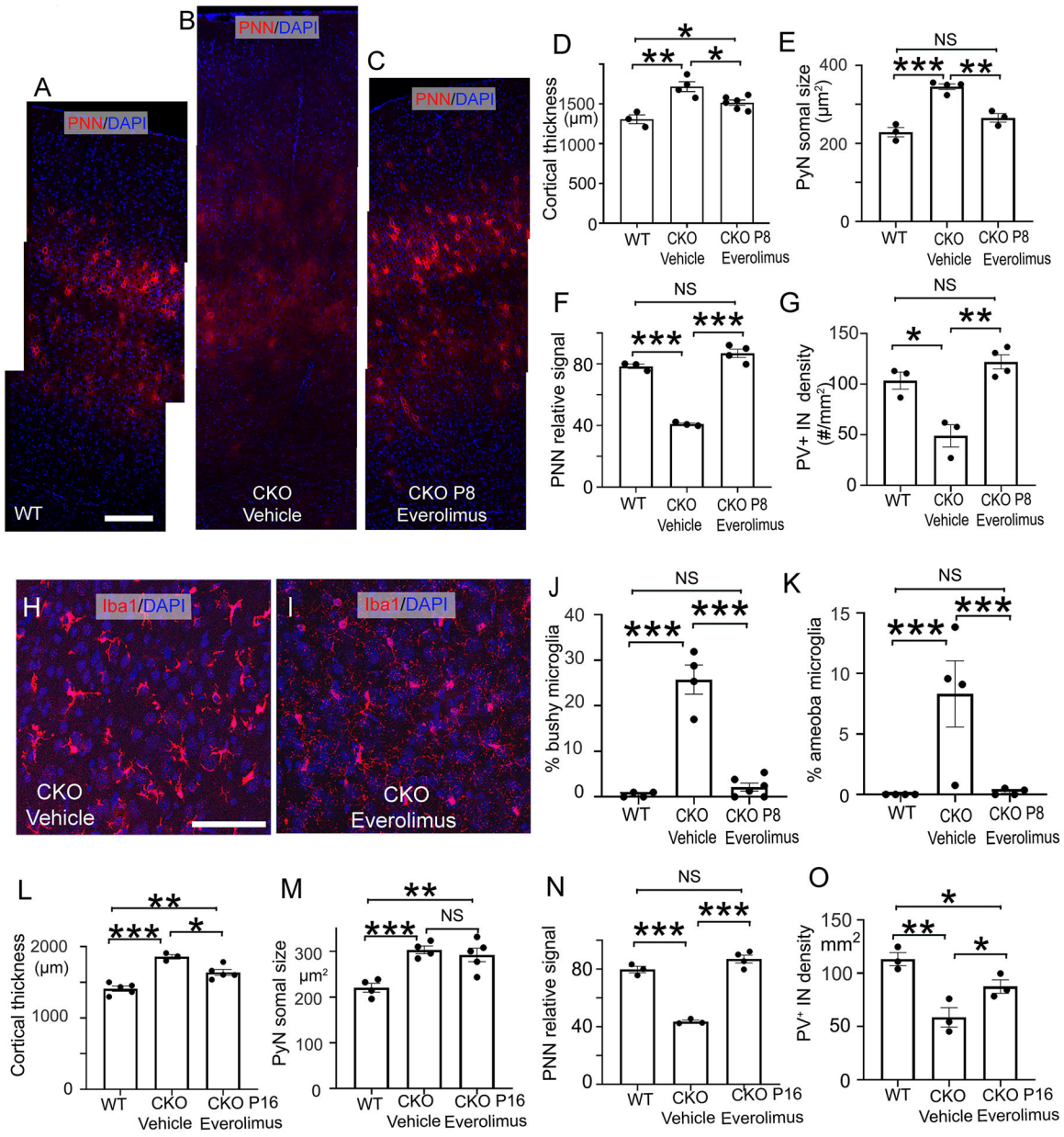

Figure 2. Everolimus rescues PNN degradation, microglial activation, and seizures.

A-C) Shown are representative images of PNN staining in A) WT, B) CKO treated with vehicle and C) CKO treated with Everolimus from P8. Early treatment partially rescues D) cortical thickness (1516.0±80.6 μm in Everolimus group, n=6 brains vs. 1717.5±123.7 μm in vehicle treatment group, n=4 brains) but completely rescues E) the soma size of pyramidal neurons (265.5±18.9 μm^2 in Everolimus group, n=3 vs. 345.3±14.6 μm^2 in the vehicle treatment group, n=4), F) WFA relative signal strength (86.9±5.5 Everolimus group n=4 vs. 40.9±1.2 in vehicle treatment group n=3), and G) PV+ cell density (122.1±14.1/mm^2 in Everolimus group, n=4 vs. 48.3±19.9/mm^2 in the vehicle treatment group, n=3). H, I) Shown are representative images of Iba1 staining in the brain of CKO without H) and with I) treatment. J-K) Quantification of J) bushy microglia (14.4±12.4% in the Everolimus

group, n=6 vs. 46.1±26.5% vehicle treatment group, n=4, and K) amoeboid microglia (2.3±4.2% in the Everolimus group, n=4 vs. 20.5±17.2% vehicle treatment group, n=4). L-O) Late Everolimus treatment partially rescues L) cortical thickness, M) soma size of mutant neurons, and O) PV+ cell density. WFA signal strength is completely rescued. Scale bar in A: 200 μm, in H: 100 μm.